

Characteristic Relations of Type-I Intermittency in the Presence of Noise

W on-Ho Kye^y and Chil-M in K in^zNational Creative Research Initiative Center for Controlling Optical Chaos,
Pai-Chai University, Taejeon 302-735, Korea

Near the point of tangent bifurcation, the scaling properties of the laminar length of type-I intermittency are investigated in the presence of noise. Based on analytic and numerical studies, we show that the scaling relation of the laminar length is dramatically deformed from $\frac{1}{\beta}$ for $\beta > 0$ to $\exp\left(\frac{1}{\beta}\right) \beta^{2/3}$ for $\beta < 0$ as β passes the bifurcation point ($\beta = 0$). The results explain why two coupled Rossler oscillators exhibit deformation of the scaling relation of the synchronous length in the nearly synchronous regime.

PACS numbers: 05.45.+b, 05.40.+j

Intermittency is the occurrence of a randomly alternating signal between long regular (laminar) phases and relatively short irregular bursts [1]. It is considered to be important as one of the routes to chaos in nonlinear dynamics. There have been extensive studies to manifest the route in terms of experiment as well as theory [1-8]. The scaling properties of the laminar length were studied for the first time by Poméau and Manneville in the Lorenz model [2]. Based on the renormalization group equation [RGE] some other authors also investigated them [5-7]. Recently, it was reported that the reinjection mechanism is another important factor that dictates the scaling relation of the laminar length [7,8].

Because noise is not avoidable in real environments, consideration of it is important to studying the realistic properties of nonlinear dynamical system [9]. The characteristics of nonlinear dynamical system in the presence of noise have been investigated by several authors based on the Fokker-Planck Equation [FPE] [3,4,7] and RGE [5,6], since the studies of Brownian motion initiated the stochastic modeling of the natural phenomena [9].

The system without noise converges to fixed points when bifurcation occurs but it does not exhibit infinite laminar phase under the succeeding random perturbation. So there is the possibility that the scaling properties show quite different features from those of the conventional ones. In this respect, the recent investigation [10] comes into our notice which observed that the scaling properties of the laminar length are deformed in the nearly synchronous regime of two coupled Rossler oscillators [11].

In this Letter, we investigate type-I intermittency in the presence of noise before and after the tangent bifurcation. Solving the Fokker-Planck equation [FPE] [4,5,9], we derive the scaling relations of the laminar length in the closed channel (i.e., $\beta < 0$) and present the results by using numerical solution and simulation. Based on them, we also explain the scaling relations that grow exponentially in the nearly synchronous regime in two coupled Rossler oscillators and eyelet intermittency [10,13].

The local Poincaré map of type-I intermittency in the

presence of noise is described as the following difference equation [1,2,4,8],

$$x_{n+1} = x_n + ax_n^2 + \sqrt{\frac{p}{2D}} \eta_n; \quad (1)$$

where a is the positive arbitrary constant, η_n the channel width between diagonal and map, and D the dispersion of Gaussian noise η_n . In the long laminar region, we can approximate the difference equation to the stochastic differential equation as follows [4]:

$$\dot{x} = -V'(x) + \sqrt{\frac{p}{2D}} \eta(t); \quad (2)$$

where dot and prime denote the differentiation with respect to t and x , respectively, $\eta(t)$ is the Gaussian white noise such that $\langle \eta(t) \rangle = 0$ and $\langle \eta(t) \eta(t') \rangle = \delta(t - t')$ [9], and $V(x)$ is the potential given by $V(x) = \frac{1}{3}ax^3 - cx + c$ where c is the integration constant. The above equation can be considered as the equation of motion of the point particle under the potential $V(x)$ and random perturbation $\eta(t)$. The relation between return map and potential is given in Fig. 1. In this figure the stable and the unstable fixed points correspond to the extremal points of the potential.

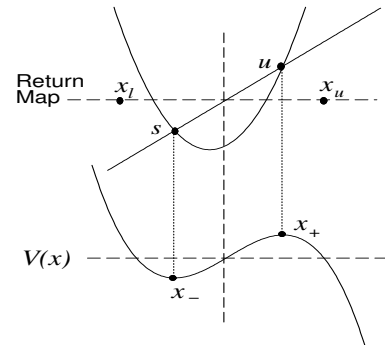


FIG. 1. The relation between fixed and extremal points for $\beta < 0$. s and u are the stable and unstable fixed points, x_l and x_u are the lower and upper bounds of laminar phase, respectively and x_- and x_+ are the extremal points of the potential.

From the above stochastic differential equation, we obtain the backward FPE [4,9] by following the well-established procedure [9] as follows:

$$\frac{\partial G(x;t)}{\partial t} = -V^0(x) \frac{\partial G(x;t)}{\partial x} + D \frac{\partial^2 G(x;t)}{\partial x^2}; \quad (3)$$

where $G(x;t)$ is the probability density of particle at $x;t$. We obtain a mean first-passage time [MFPT] equation after integrating the above FPE with respect to time as follows [4,9]:

$$1 = -V^0(x) \frac{dT}{dx} + D \frac{d^2 T}{dx^2}; \quad (4)$$

where $T(x)$ is the mean escaping time defined by $T(x) = \int_0^\infty t \frac{\partial G(x;t)}{\partial t} dt$ under the boundary conditions that $G(x;0) = 1$ and $\lim_{t \rightarrow \infty} G(x;t) = 0$. The MFPT function $T(x)$ is the average transition time from the reinjection to the escaping point of the particle under the potential $V(x)$ and random perturbation.

The general solution of Eq. (3) can be derived as follows:

$$T(x) = c \int_{x_1}^x dx^0 \exp \left[-\frac{1}{D} \int_{x_1}^{x^0} V(x^0) dx^0 \right] + \frac{1}{D} \int_{x_1}^x dx^0 \exp \left[-\frac{1}{D} \int_{x_1}^{x^0} V(x^0) dx^0 \right] \int_{x_1}^{x^0} dx^0 \exp \left[\frac{1}{D} \int_{x_1}^{x^0} V(x^0) dx^0 \right]; \quad (5)$$

where c is the integration constant, x_1 is the lower bound of the laminar phase, and x is the destination point of the transition. We can easily verify that Eq. (5) is the general solution for the MFPT equation by inserting Eq. (5) into Eq. (4).

If noise is small enough such that $D \ll 1$, the first term in the above equation is suppressed by the factor of $1=D$ and the second term becomes dominant. The second term is not integrable analytically. Then we can expand the potential at the extremal point x_{approx} approximately (see Fig. 1) such that $V(x) = V(x_{\text{approx}}) + \frac{V''(x_{\text{approx}})}{2} (x - x_{\text{approx}})^2 + O((x - x_{\text{approx}})^3)$.

In that case, the MFPT function $T(x)$ can be approximated as follows:

$$T(x) = \frac{1}{D} \exp \left[-\frac{1}{D} \int_{x_1}^x V(x^0) dx^0 \right] + \frac{1}{2D} V''(x_{\text{approx}}) (x - x_{\text{approx}})^2 \exp \left[-\frac{1}{D} \int_{x_1}^x V(x^0) dx^0 \right]; \quad (6)$$

The extremal points are given by $x_{\text{approx}} = x_{\text{approx}}$ in Eq. (2). In the far outside of the laminar phase (i.e., at the limit $x \rightarrow 1$ and $x_1 \rightarrow x$), we can perform the integration of the quadratic exponent [9] and then obtain the following approximated solution of the MFPT equation:

$$T \approx \frac{1}{a} \exp \left[-\frac{4}{3D} \left(\frac{x}{a} \right)^3 \right] \quad \text{for } x < 0; \quad (7)$$

The above solution is consistent with the formal one which was derived in the previous investigation by the FPE and RGE analysis [3,5,7] such that $\ln T \approx \ln \left(\frac{1}{a} \right) - \frac{4}{3D} \left(\frac{x}{a} \right)^3$. We remark the fact that there has been no explicit derivation in analytic form like Eq. (7). The analytic solution is important in analyzing various intermittent phenomena quantitatively. In particular we are interested in the mysterious deformation of the type-I scaling near phase synchronization regime [10] and eventually show that it enables the theoretical understanding of those phenomena.

After taking the logarithm on Eq. (7), we obtain the equation such that $\ln T \approx \ln \left(\frac{1}{a} \right) - \frac{4}{3D} \left(\frac{x}{a} \right)^3$. Our main interests are in the far region ($x \rightarrow 0$) from the bifurcation point because the transition from the intermittency to stable orbit occurs here. In this region the scaling is dominated by the second term such that $\ln T \approx -\frac{4}{3D} \left(\frac{x}{a} \right)^3$ (note that this exponential saturation rapidly forms from $x \approx 10^{-3}$ because the noise is small enough such that $\frac{1}{D} = 0.5 \times 10^6$ in our simulation (see Fig. 3 (b))).

The reinjection probability $P(x_{\text{in}})$ was reported to be another important factor which affects the scaling relations of the laminar length [8]. And it was generally considered to obtain average laminar length [7,8]. But in this investigation we only consider the fixed reinjection probability $P(x_{\text{in}}) = P(x_{\text{in}})$ to study the intrinsic scaling property of the system (note in all of our simulation we set the reinjection point $x_{\text{in}} = x_1$).

Note that the approximation procedure used in Eq. (6) is not applicable for $x > 0$ and a transient region because the equation is a solution for $x < 0$ where the potential has extremal points (see Fig. 1). At the far outside from the bifurcation point (i.e., $D > 0$), we take the limit $D \rightarrow 0$ in Eq. (4) and obtain the conventional scaling relation of type-I intermittency $T \approx \frac{1}{D}$ [2,4]. For intermediate range D , we present the numerical results of the scaling relation of the laminar length in Fig. 3 (c) and (d).

In Eq. (7), if we take $D \rightarrow 0$ the MFPT function $T \rightarrow 1$. So the particle trapped in the well does not escape from it if the random perturbation is turned off.

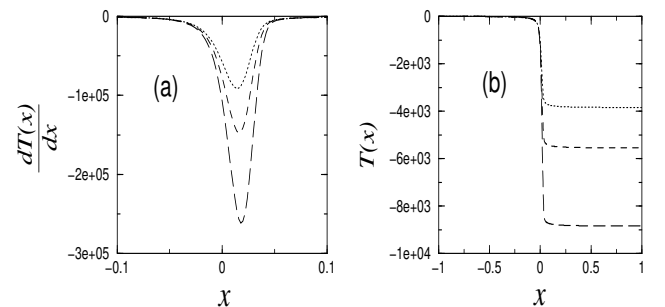


FIG. 2. The numerical solutions of the MFPT equation. (a) the first differentiation of the MFPT function and (b) the MFPT function when $a = 0.1$ and $D = 2.0 \times 10^{-6}$. The dotted, dashed, and long dashed lines are for $\epsilon = 1.0 \times 10^{-5}$; $\epsilon = 2.0 \times 10^{-5}$; and $\epsilon = 3.0 \times 10^{-5}$; respectively.

The scaling relation of the laminar length can be verified in numerical solutions and simulations. In Fig. 2, the numerically solved the MFPT function $T(x)$ shows the typical kink shape [14], thus we can know that $T(x)$ is the good physical quantity reflecting the transition characteristics of intermittency from the laminar phase to chaotic burst. In that case we can define a topological index of the transition such that $Q = \int T(1) - T(-1) dx$ [14]. The negative signature in Fig. 1 stems from the backwarding property of FPE of Eq. (3) and the absolute value of the MFPT function $T(x)$ is the laminar length [4,9].

In the following presentation of the numerical results, we let $x_1 = -1.0$ and $x_2 = 1.0$ and the average laminar length is $hli = \int_{-1}^1 T(x) dx$ (as given in Fig. 2 (b)), $T(x)$ rapidly converges to the constants outside the center, so that we can say that hli is a kind of topological index as defined above). To confirm the scaling relation of Eq. (7), we not only perform a direct simulation with Eq. (1) but also solve the second order MFPT equation (Eq. (4)) numerically.

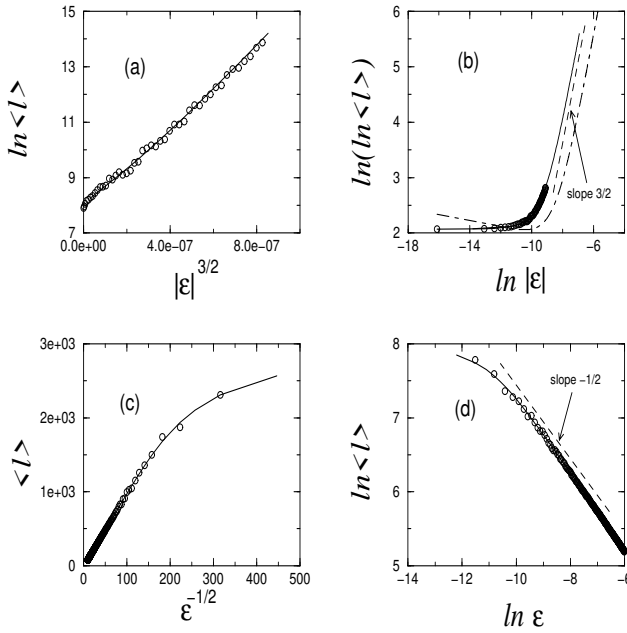


FIG. 3. The laminar scaling before and after the tangent bifurcation. (a) and (b) are for $\epsilon < 0$. (c) and (d) are for $\epsilon > 0$. The circles are simulation data from Eq. (1) and the solid lines are solution data from Eq. (4). The dashed lines in (b) and (d) show the slope 3/2 and -1/2 saturation, respectively and the dot-dashed line in (b) is an analytic solution curve (Eq. (7)) (the maximum and dispersion of the Gaussian noise are $j = 2.0 \times 10^{-3}$ and $D = 2.0 \times 10^{-6}$, respectively).

In Fig. 3, the circle points and solid lines are simulation data from Eq. (1) and solution data from Eq. (4), respectively. The dashed lines in Fig. 3 (b) and (d) are 3=2 scaling expected from Eq. (7) and 1=2 scaling for $\epsilon > 0$, respectively. When we simulate Eq. (1), the approximated Gaussian noise is used (see the caption of Fig. 3 for details). The solution data agree well with the simulation ones. We note here that there are some shifts from the solution line when the uniform noise is applied, but the scaling behaviors are invariant in both cases.

Fig. 3 (a) shows the scaling relation for $\epsilon < 0$. The figure, $\ln hli$ as a function of $j^{3/2}$ shows a straight line approximately to confirm $hli \propto \exp \frac{1}{j^{3/2}}$. The exponent 3=2 appears more clearly when we obtain $\ln(hli)$ as a function of $\ln(\epsilon)$ as given in Fig. 3 (b). Thus we can verify the slope is eventually saturated to 3=2. This is the very scaling behavior obtained in Eq. (7) analytically. The analytic solution is also given in Fig. 3 (b) as the dot-dashed line that is the plotting of Eq. (7). In figures though we present the simulation data within the limit of numerical calculation of the map (Eq. (1)) the data well follow the deformation of the scaling behavior.

In Fig. 3 (c), the conventional scaling $hli \propto \epsilon^{-1/2}$ holds for relatively wide channel region ($\epsilon > 0$) so that the slope -1/2 saturation can be obtained in Fig. 3 (d). As the channel width becomes close to zero, the straight line begins to bend (Fig. 3 (c)) and after it passes zero point, the straight line reappears (Fig. 3 (a)).

We now apply this analysis to two coupled Rossler oscillators which are a good laboratory for the studying of type-I intermittency with random perturbation [10,12]. It is important to discuss the correspondence between two coupled Rossler oscillators and type-I intermittency in the presence of noise to explore the origin of nearly synchronous phenomena. The two coupled Rossler oscillators are given as follows [10,12]:

$$\begin{aligned} \dot{x}_{1,2} &= -x_{1,2}y_{1,2} - z_{1,2} + (x_{2,1} - x_{1,2}); \\ \dot{y}_{1,2} &= x_{1,2}x_{1,2} + 0.15y_{1,2}; \\ \dot{z}_{1,2} &= 0.2 + z_{1,2}(x_{1,2} - 10.0); \end{aligned} \quad (8)$$

where $x_{1,2} = 1.0 - 0.015$. The phase difference between the two oscillators can be rewritten as follows:

$$\frac{d}{dt}(\phi) = F(\phi; \epsilon) + G(\phi; \epsilon); \quad (9)$$

where,

$$\begin{aligned} F(\phi; \epsilon) &= -\phi_1 - \phi_2 - \frac{1}{2} \left[\frac{A_2}{A_1} + \frac{A_1}{A_2} \right] \sin \phi; \\ G(\phi; \epsilon) &= 0.15(\sin \phi_1 \cos \phi_1 - \sin \phi_2 \cos \phi_2) \\ &\quad + \left(\frac{z_1}{A_1} \sin \phi_1 - \frac{z_2}{A_2} \sin \phi_2 \right); \end{aligned}$$

where $\phi = \phi_1 - \phi_2$, $A_{1,2} = \sqrt{x_{1,2}^2 + y_{1,2}^2}$ and $\phi_{1,2} = \arctan(y_{1,2}/x_{1,2})$. In the above equations we neglect the

fast actuation term which depends on ϵ , in $F(\epsilon; \epsilon)$ as discussed in Ref. [10].

As already discussed in Ref. [10], the potential of this system $V(\epsilon) = -\int dF(\epsilon; \epsilon)$ shows the saddle node bifurcation at $\epsilon_t (= 0.0276)$. If we identify $G(\epsilon_1; \epsilon_2)$ as the random perturbation term of Eq. (1), we can argue the scaling relation of the length of synchronization in nearly synchronous regime of these two coupled oscillators are effectively similar to that of type-I intermittency with noise (Eq. (2)) (note: the dispersion of $G(\epsilon_1; \epsilon_2)$ hardly depends on ϵ for $\epsilon_t < \epsilon < \epsilon_c$). Thus we remark the scaling of the laminar length is separated into two regions in the center of $\epsilon = \epsilon_t$. So it has $h_{li} \sim \exp f_j \epsilon^{-3/2} g$ for $\epsilon > \epsilon_t$ and $h_{li} \sim j \epsilon^{-1/2}$ for $\epsilon < \epsilon_t$ like the previously presented results (note: based on numerical studies, Ref. [10] proposed the scaling $h_{li} \sim \exp f_j \epsilon^{-1/2} g$ for $\epsilon > \epsilon_t$ ($\epsilon_c = 0.0286$)).

As in the above analysis, the persistency of the intermittency is caused by the random perturbation $\epsilon(t)$ in closed channel region. Thus it can be argued that the nontrivial 2 phase jumps observed in Ref. [10] originates from the random perturbation term $G(\epsilon_1; \epsilon_2)$, neglected in the discussion of Ref. [10], rather than from the term $\frac{A_2}{A_1} + \frac{A_1}{A_2}$. We perform the numerical simulation for the scaling of the laminar length in both regions ($\epsilon < \epsilon_t$ and $\epsilon > \epsilon_t$), and the results are presented in the Fig. 4. As we expected, the figures well agree with the previous theoretical analysis of the scaling relation.

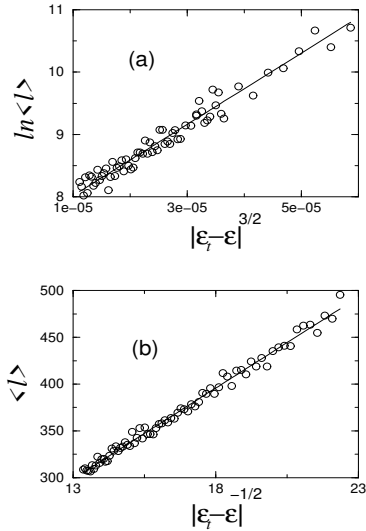


FIG. 4. The laminar scaling in the two coupled Rossler oscillators for (a) $\epsilon > \epsilon_t$ and (b) $\epsilon < \epsilon_t$.

In conclusion, the new scaling relation of type-I intermittency is presented in the region after the tangent bifurcation. We observe that the conventional scaling relation $h_{li} \sim \epsilon^{-1/2}$ of type-I intermittency holds only in relatively wide channel ($\epsilon - \epsilon_t > 0$) and it begins to deform as ϵ approaches zero. The scaling relation is eventually saturated by $h_{li} \sim \exp f_j \epsilon^{-3/2} g$ (Eq. (7) and Fig 3. (a)

and (b)) after the tangent bifurcation ($\epsilon < 0$). Such dramatic deformation of the scaling relation stems from the persistency of the intermittency with the random perturbation even though the system is in a state of closed channel region (i.e., $\epsilon < 0$). This is why the laminar length in closed channel region grows faster than that of the positive one [12,13]. From these results, we can also explain why two coupled Rossler oscillators exhibit deformation of the scaling relation of the synchronous length in the nearly synchronous regime [10].

The authors thank J. P. Eckmann and P. Wittwer for helpful comments and S. Rim, D. U. Hwang, and I. B. Kim for valuable discussions. This work is supported by Creative Research Initiatives of the Korea Ministry of Science and Technology.

^y Electronic address: whkye@alpha.paichai.ac.kr

^z Electronic address: rchm.kim@mailpaichai.ac.kr

- [1] E. Ott, Chaos in dynamical systems, (Cambridge University Press, 1993).
- [2] P. Manneville and Y. Pomeau, Phys. Lett. 75A, 1 (1979).
- [3] J. P. Eckmann, L. Thomas and P. Wittwer, J. Phys. A 14, 3153 (1982).
- [4] J. E. Hirsch, B. A. Huberman, and D. J. Scalapino, Phys. Rev. A 25, 519 (1982).
- [5] J. E. Hirsch, M. Nauenberg, and D. J. Scalapino, Phys. Lett. 87A, 391 (1982).
- [6] B. Hu and J. Rudnick, Phys. Rev. Lett. 48, 1645 (1982); O. J. Kwon, C. M. Kim, E. K. Lee, and H. Lee, Phys. Rev. E 53, 1253 (1996).
- [7] J. P. Cuthrell, J. D. Farmer, and B. A. Huberman, Phys. Rep. 92, 45 (1982).
- [8] C. M. Kim, O. J. Kwon, E. K. Lee, and H. Y. Lee, Phys. Rev. Lett. 73, 525 (1994); C. M. Kim, G. S. Yim, J. W. Ryu, and Y. J. Park, Phys. Rev. Lett. 80, 5317 (1998).
- [9] C. W. Gardiner, Handbook of Stochastic Methods (Springer-Verlag, 1985), Second Edition; H. Risken, The Fokker-Planck Equation (Springer-Verlag, 1996) second edition (for the correspondence between stochastic differential equation and FPE, see those sections 3.6, 4.3 and 5.2 of the first book).
- [10] K. J. Lee, Y. Kwak, and T. K. Lim, Phys. Rev. Lett. 81, 321 (1998).
- [11] M. G. Rosenblum, A. S. Pikovsky, and J. Kurths, Phys. Rev. Lett. 76, 1804 (1996).
- [12] A. S. Pikovsky, M. Rosenblum, G. V. Osipov, M. Zaks, and J. Kurths, Physica D 104, 219 (1997).
- [13] C. Grebogi, E. Ott and J. A. Yorke, Phys. Rev. Lett. 50, 935 (1983); A. S. Pikovsky, G. Osipov, M. Rosenblum, M. Zaks, and J. Kurths, Phys. Rev. Lett. 79, 47 (1997).
- [14] R. Rajaraman, Solitons and Instantons (North-Holland, 1982).